Fluid Phase Equilibria 345 (2013) 60–67

Contents lists available at SciVerse ScienceDirect

Fluid Phase Equilibria

journal homepage: www.elsevier.com/locate/fluid

Isobaric vapor–liquid equilibrium and isothermal surface tensions of 2,2′-oxybis[propane] + 2,5-Dimethylfuran

Andrés Mejía[a,*], Mariana B. Oliveira[b], Hugo Segura[a], Marcela Cartes[a], João A.P. Coutinho[b]

[a] Departamento de Ingeniería Química, Universidad de Concepción POB 160 – C, Correo 3, Concepción, Chile
[b] Departamento de Química, CICECO, Universidade de Aveiro, Campus Universitário de Santiago, 3810-193 Aveiro, Portugal

ARTICLE INFO

Article history:
Received 30 November 2012
Received in revised form 31 January 2013
Accepted 6 February 2013
Available online 20 February 2013

Keywords:
Vapor–liquid equilibrium
Surface tension
Square gradient theory
CPA EoS
2,2′-Oxybis[propane] or DIPE
2,5-Dimethylfuran or DMF

ABSTRACT

Isobaric vapor–liquid equilibrium (VLE) data have been measured for the binary system 2,2′-oxybis[propane] + 2,5-Dimethylfuran at 50, 75, and 94 kPa and over the temperature range 321–364 K using a vapor–liquid equilibrium still with circulation of both phases. Atmospheric surface tension (ST) data have been also determined at 283.15 and 330.15 K using a maximum bubble pressure tensiometer. Experimental results show that the mixture is zeotropic and exhibits slight positive deviation from ideal behavior over the experimental range. Surface tensions, in turn, exhibit negative deviation from the linear behavior. For each isothermal condition, it is observed that the surface tension decreases as the mole fraction of 2,2′-oxybis[propane] increases, whereas at a fixed mole fraction, the surface tension decreases as the temperature increases.

The VLE data of the binary mixture satisfy the Fredenlund's consistency test, and the dependence of ST on mole fraction was satisfactorily smoothed using the Redlich–Kister equation.

The experimental VLE and ST data were accurately described by applying the square gradient theory to the Cubic-Plus-Association equation of state. This theoretical model was also applied to describe the surface activity of species along the interfacial region, from which it is possible to conclude that only the 2,2′-oxybis[propane] presents an interfacial accumulation which decreases as the concentration of DIPE or temperature increases.

1. Introduction

During the last years renewable source of fuels have gained importance due to the need to find environmental friendly and sustainable fuels. One promising new fuel is 2,5-Dimethylfuran (or DMF). Technically, DMF exhibits some interesting fuel features, such as an energy density similar to gasoline and 40% superior to ethanol [1], a Research Octane Number (RON) similar to gasoline and ethanol [2], and a stoichiometric air/fuel ratio lower than the stoichiometric air/fuel ratio of gasoline. In practice, DMF has been successfully tested as a fuel in a direct-injection spark-ignition engine, showing an excellent performance [3–5]. Additionally, among its attributes, DMF can be obtained from fructose through a high yield chemical or biochemical route (catalytic biomass-to-liquid process) where the raw material is fructose, which can be obtained from fruit, some root vegetables or sucrose [2].

In order to explore DMF applications as a fuel or as a gasoline additive, it is necessary to characterize its thermo-physical properties, such as the vapor–liquid equilibrium, density, and surface tension as a pure fluid as well as mixed with hydrocarbons or other gasoline additives, such as ethers and alcohols. In spite of their importance, experimental and theoretical investigations concerning key properties such as vapor–liquid equilibrium (VLE) and surface tension (ST) are scarce and limited to narrow experimental conditions. To the best of our knowledge, the available experimental data for DMF is scarce and limited to pure fluid vapor pressures [6], densities [6,7] and surface tensions [8]. For the case of DMF based mixtures, only VLE, mixing volumes and ST data have been reported by us for DMF + hexane [8].

Consequently, and as part of our ongoing research program devoted to the characterization of the thermo-physical properties of DMF mixtures, this work is undertaken to determine VLE and ST data of 2,2′-oxybis[propane] (or DIPE) + DMF and to analyze its phase and interface behavior under the light of molecular theories. Specifically, a primary goal of this contribution is to report isobaric VLE data at 50, 75 and 94 kPa for DIPE + DMF, together with their atmospheric ST at 283.15 and 330.15 K. An additional goal is to simultaneously describe both bulk phase (VLE) and interfacial properties (ST and surface activity) of the mixture. For that purpose, bulk phases are described by using the Cubic-Plus-Association (CPA) EoS [9–13] while the corresponding interfacial properties are predicted by applying the square gradient theory (SGT) [14] to that

* Corresponding author. Tel.: +56 41204534; fax: +56 41247491.
E-mail address: amejia@udec.cl (A. Mejía).

0378-3812/$ – see front matter © 2013 Elsevier B.V. All rights reserved.
http://dx.doi.org/10.1016/j.fluid.2013.02.005

List of symbols

a	cohesion parameter in the EoS
$a_{o,i}$	pure compound parameter in the EoS
A_i, B_i, C_i	Antoine constants in Eq. (4)
b_i	covolume parameter in the EoS
B	second virial coefficients of the pure gases
c_i	influence parameter
$c_{1,i}$	pure compound parameter in the EoS
c_k	Redlich–Kister parameters
f_0	Helmholtz energy density of the homogeneous system
g	simplified radial distribution function
k	binary interaction parameter
m	number of parameter in Redlich–Kister expansion
nc	number of components
n_D	refractive index
p	absolute pressure
r_i	radii of probe orifice i
R	universal gas constant
T	absolute temperature
T_b	normal boiling temperature
V	volume
v	voltage
x, y	mole fraction of the liquid and vapor phases
X_{A_i}	mole fraction of pure component i not bonded at site A

Greek

$\beta^{A_iB_i}$	association volume parameter
δ	mixing rule of second virial coefficients
Δ	differential
$\Delta^{A_iB_j}$	association strength
$\varepsilon^{A_iB_i}$	association energy parameter
γ	activity coefficient
μ	chemical potential
$\hat{\rho}$	mass density
ρ	molar density
σ	surface tension

Subscripts

1, 2	number of orifice
c	critical state
exp	experimental
i, j	components i, j respectively
r	reduced property

Superscripts

lit	literature
L	Liquid
V	Vapor
0	Equilibrium

EoS model. As we have demonstrated in previous works ([15–22], and references therein), such a modeling approach provides a full predictive scheme both for bulk and interfacial properties from experimental VLE values and surface tensions of the pure components.

2. Experimental

2.1. Purity of materials

2,2′-Oxybis[propane] and 2,5-Dimethylfuran were purchased from Merck and Aldrich, respectively. Both chemicals were used without further purification. Table 1 reports the purity of the components (as determined by gas chromatography, GC), together with the normal boiling points (T_b), the mass densities ($\hat{\rho}$), the refractive indexes (n_D) at 298.15 K and the surface tensions (σ) of pure fluids at 303.15 K. The reported values are also compared with those previously reported [8,23].

2.2. Apparatus and procedure

2.2.1. Vapor–liquid equilibrium cell

An all-glass vapor–liquid equilibrium apparatus model 601, manufactured by Fischer Labor and Verfahrenstechnik (Germany), was used in the equilibrium determinations. In this circulation-method apparatus, the mixture is heated to its boiling point by a 250 W immersion heater. The vapor–liquid mixture flows through an extended contact line (Cottrell pump) that guarantees an intense phase exchange and then enters to a separation chamber whose construction prevents an entrainment of liquid particles into the vapor phase. The separated gas and liquid phases are condensed and returned to a mixing chamber, where they are stirred by a magnetic stirrer, and returned again to the immersion heater. The temperature in the VLE still was determined with a Systemteknik S1224 digital temperature meter and a Pt 100 probe, which was calibrated against the experimental fusion and boiling points of distilled water. The reliability of such a calibration procedure was successfully checked using the experimental boiling temperature data of the pure fluids used in this work. The accuracy is estimated as ±0.02 K. The total pressure of the system is controlled by a vacuum pump capable of work under vacuum up to 0.25 kPa. The pressure is measured with a Fischer pressure transducer calibrated against an absolute mercury-in-glass manometer (22 mm diameter precision tubing with cathetometer reading); the overall accuracy is estimated as ±0.03 kPa.

On average the system reaches equilibrium conditions after (2–3) hours operation. The 1.0 μL samples taken by syringe after the system had achieved equilibrium and were analyzed by gas chromatography on a Varian 3400 apparatus provided with a thermal conductivity detector and a Thermo Separation Products model SP4400 electronic integrator. The column was 3 m long and 0.3 cm in external diameter, packed with SE-30. Column, injector, and detector temperatures were 343.15, 433.15, and 493.15 K, respectively. Good separation was achieved under these conditions, and calibration analyses were carried out to convert the peak area ratio to the mass composition of the sample. The pertinent polynomial fit of the calibration data had a correlation coefficient R^2 better than 0.99. At least three analyses were made of each sample. The maximum standard deviation of these analyses was 0.002 in area percentage. Concentration measurements were accurate to better than ±0.001 in mole fraction. Additional details concerning low pressure vapor–liquid measurements have been described in depth by Raal and Ramjugernath [24].

2.2.2. Density and refractive indexes measurements

The mass density ($\hat{\rho}$) of the pure fluids was measured at 298.15 K using a DMA 5000 densimeter (Anton Paar, Austria) with an accuracy of 5×10^{-6} g cm^{-3}. The density determination is based on measuring the period of oscillation of a vibrating U-shaped tube filled with the liquid sample. During the operation, the temperature of the apparatus was maintained constant to within ±0.01 K. The refractive indexes (n_D) of pure liquids were measured at 298.15 K

Table 1
Gas chromatography (GC) purities (mass fraction), refractive index (n_D) at Na D line, mass densities ($\hat{\rho}$), normal boiling points (T_b) and surface tensions (σ) of pure components.[a]

Component (purity/mass fraction)	n_D T (K) = 298.15		$\hat{\rho}$ (g cm^{-3}) T (K) = 298.15		T_b (K) p (kPa) = 101.33		σ (mN m^{-1}) T (K) = 303.15	
	Exp.	Lit.	Exp.	Lit.	Exp.	Lit.	Exp.	Lit.
2,2′-Oxybis[propane] or DIPE (0.999)	1.36652	1.36644[b]	0.71875	0.71834[b]	341.67	341.60[b]	16.70	16.70[b]
2,5-Dimethylfuran or DMF (0.999)	1.44012	1.44040[c]	0.89563	0.89579[d]	366.83	366.83[c]	24.05	24.04[c]

[a] The measurement uncertainties are: $n_D \pm 10^{-5}$; $\hat{\rho} \pm 5 \times 10^{-6}$ g cm^{-3}; $\sigma \pm 0.01$ mN m^{-1}; $p \pm 0.03$ kPa; $T \pm 0.01$ K.
[b] Mejía et al. [23].
[c] Mejía et al. [8].
[d] Interpolated from Mejía et al. [8].

using a Multiscale Automatic Refractometer RFM 81 (Bellingham + Stanley, England). During the operation, temperature was controlled to within ±0.01 K by means of a thermostatic bath (Haake DC3, Germany). The uncertainties in refractive index measurements are $\pm 10^{-5}$.

2.2.3. Surface tension measurements

A maximum differential bubble pressure tensiometer model PC500-LV manufactured by Sensadyne Inc. (USA), was used in surface tension measurements. In this equipment, two glass probes of different orifice radii ($r_1 = 0.125 \pm 0.01$ mm and $r_2 = 2.0 \pm 0.01$ mm) are immersed in a vessel that contains the sample to be measured. In order to guarantee high accuracy and reduce the measurement errors, the glass probe with the small orifice was located 2.5 mm below the probe with the larger orifice. Ultra high purity nitrogen (UHP = 99.995%) is then blown through the probes and the differential pressure (Δp) between them is recorded.

According to the Laplace's equation, Δp and r_1, r_2 are related to the surface tension, σ, as:

$$\Delta p = p_1 - p_2 = 2\sigma(r_1^{-1} - r_2^{-1}) \quad (1)$$

where p_i is the pressure exerted by the gas flow in the probe of radius r_i. The gas flow is controlled by a sensor unit connected to a personal computer through an interface board (PCI-DAS08, Measurement Computing, USA). Besides a constant volume flow controller, this sensor unit contains a differential pressure transducer, a temperature transducer and a pressure regulator. The temperature of the sample in the vessel is measured by means of a Pt 100 probe, and maintained constant to within ±0.01 K using a thermostatic bath (Julabo, Germany).

The experimental method for determining surface tensions proceeds as follows: the mixture to be analyzed is prepared by adding appropriate volumes of each pure fluid. The sample is then placed into the vessel, where it is heated to the experimental temperature and stirred during 5 min by a magnetic stirrer. At that moment, the concentration of the sample is determined in triplicate by means of GC. Thereafter, UHP nitrogen flows through the probes, and the sensor unit translates the measurement of voltage signal (Δv) to a Δp signal. The relation between $\Delta v - \Delta p$ is obtained by calibrating the sensor unit software using two reference fluids with well-characterized surface tensions over the range of expected measurements. In this work, we used de-ionized water as the high surface tension reference fluid, while ethanol as low surface tension reference fluid. Finally, the surface tension is calculated from the Sensadyne software according to Eq. (1) within ±0.01 mN m^{-1}. This calculation is carried out for a mixture of constant concentration, and over a period of time where the surface tension reaches a static or constant value.

As part of the experimental procedure, the probes are periodically cleaned before each experimental measurement. The cleaning procedure consists in washing the probes with acetone and then, in drying them with additive-free wipes (Kimwipes, Kimberly–Clark Co.), and nitrogen. Additional details concerning to the maximum differential bubble pressure technique have been extensively described by Evans [25].

3. Theoretical section

3.1. Experimental data treatment and consistency

Isobaric VLE measurements have been used to predict the activity coefficients (γ_i) and then to evaluate their consistency. γ_i are calculated from the following equation: [26]

$$\ln \gamma_i = \ln \frac{y_i p}{x_i p_i^0} + \frac{(B_{ii} - V_i^L)(p - p_i^0)}{RT} + y_j^2 \frac{\delta_{ij} p}{RT} \quad (2)$$

where p is the total pressure and p_i^0 is the pure component vapor pressure. R is the universal gas constant. T is the equilibrium temperature. x_i and y_i are the mole fraction of the liquid and the vapor-phase of component i, respectively. V_i^L is the liquid molar volume of component i, B_{ii} and B_{jj} are the second virial coefficients of the pure gases, B_{ij} is the cross second virial coefficient, and the mixing rule of second virial coefficients (δ_{ij}) is given by

$$\delta_{ij} = 2B_{ij} - B_{jj} - B_{ii} \quad (3)$$

According to Eq. (2), the standard state for calculating activity coefficients is the pure component at the pressure and temperature of the solution. Eq. (2) is valid from low to moderate pressures, where the virial equation of state truncated after the second term is adequate for describing the vapor phase of the pure components and their mixtures and, additionally, the liquid molar volumes of pure components are incompressible over the pressure range under consideration. In this work, liquid molar volumes are estimated from the correlation proposed by Rackett [27]. The molar virial coefficients B_{ii}, B_{jj} and B_{ij} were estimated by the method of Tsonopoulos [28]. The vapor pressure of 2,2′-oxybis[propane] was experimentally determined as a function of temperature using the same equipment as that for obtaining the VLE data, and the temperature dependence of p_i^0 is then correlated using the Antoine equation:

$$\log(p_i^0/\text{kPa}) = A_i - \frac{B_i}{(T/\text{K}) + C_i} \quad (4)$$

where A_i, B_i, and C_i are the Antoine constants. For the case of 2,5-Dimethylfuran, Antoine's constants were taken from Ref. [8].

In order to test the thermodynamic consistency of the present VLE data, we applied the point-to-point method of Van Ness et al. [29] as modified by Fredenslund et al. [30]. In the latter approach, an isobaric VLE dataset is consistent when an average deviation of $\Delta y < 0.01$ is met by fitting the equilibrium vapor pressure according to the Barker's [31] reduction method.

Isothermal experimental data of the surface tension (σ) have been correlated by using the Redlich–Kister expansion: [32]

$$\sigma = x_1 x_2 \sum_{k=0}^{m} c_k (x_2 - x_1)^k + x_1\sigma_1 + x_2\sigma_2 \quad (5)$$

where m denotes the number of c_k parameters, which can be found by a Simplex optimization technique. σ_i denotes the surface tension of the pure components.

3.2. Modeling of phase equilibrium and interfacial behavior

Simultaneous modeling of VLE and IFT for fluid mixtures is carried out by applying the square gradient theory (SGT). According to the SGT, the isothermal surface tension of a binary mixture, σ, is given by the following integral expression: [15,33]

$$\sigma = \sqrt{2}\int_{\rho_2^v}^{\rho_2^L} \sqrt{(f_0 - (\rho_1\mu_1^0 + \rho\mu_2^0) + p^0)\left(c_{22} + 2\sqrt{c_{11}c_{22}}\frac{d\rho_1}{d\rho_2} + c_{11}\left(\frac{d\rho_1}{d\rho_2}\right)\right)}\, d\rho_2 \tag{6}$$

where f_0 is the Helmholtz energy density of the homogeneous system, ρ_i is the interfacial molar concentration of species i. ρ_i^V and ρ_i^L corresponds to the molar concentration of component i in the V and L bulk equilibrium phases, respectively. μ_i is the chemical potential of species i. The superscript 0 in μ_i denotes that it is evaluated at the phase equilibrium condition of the bulk phases (V, L). p^0 is the phase equilibrium pressure, and c_{ii} is the influence parameter of species i.

Within the theoretical framework of the SGT, the isothermal bulk phase equilibrium properties (i.e. ρ_i^V, ρ_i^L, and p^0) are found by solving the following conditions at bulk phases [15]

$$f_0 - (\rho_1\mu_1^0 + \rho_2\mu_2^0) + p^0 = 0 \tag{7.a}$$

$$\left(\frac{\partial f_0}{\partial \rho_i}\right)_{T^0,V^0,\rho^0_{k\neq i}} - \mu_i^0 = \mu_i - \mu_i^0 = 0 \quad i = 1,2 \tag{7.b}$$

$$\left(\frac{\partial^2 f_0}{\partial \rho_i^2}\right)_{T^0,V^0,\rho^0_{k\neq i}} = \left(\frac{\partial \mu_i}{\partial \rho_i}\right)_{T^0,V^0,\rho^0_{k\neq i}} > 0 \quad i = 1,2 \tag{7.c}$$

Eqs. (7.a)–(7.c) are equivalent to the necessary conditions of phase equilibrium for bulk phases. Specifically, Eq. (7.a) corresponds to the mechanical equilibrium condition ($p^L = p^V = p^0$) while Eq. (7.b) expresses the chemical potential constraint ($\mu_i^L = \mu_i^V = \mu_i^0$). Eq. (7.c) is a differential stability condition for interfaces, comparable to the Gibbs energy stability constraint of a single phase [34].

The influence parameter of species c_{ii} and c_{jj} can be calculated at the boiling temperature from experimental σ values (σ_{exp}) and Eq. (6) for the case a pure fluid [15,16,18–20,33]:

$$c_{ii}(T^0) = \sigma_{exp}^2(T^0)\left(\int_{\rho_i^V}^{\rho_i^L}\sqrt{2(f_0 - \rho_i\mu_i^0 + p^0)}d\rho_i\right)^{-2} \tag{8}$$

For the case of 2,5-Dimethylfuran, σ_{exp} data have been taken from Ref. [8] whereas σ_{exp} data for 2,2′-oxybis[propane] have been taken from the Daubert and Danner data base [35].

Following the SGT, ρ_1 and ρ_2 in Eq. (6) are implicitly related by the following algebraic equation:

$$\sqrt{c_{11}}(\mu_2 - \mu_2^0) = \sqrt{c_{22}}(\mu_1 - \mu_1^0) \tag{9}$$

Eqs. (6)–(9) are the main expression of the SGT needed to simultaneous modeling of VLE and ST. In the latter equations, f_0 and μ_i can be obtained from any EoS. In this work, f_0 and its density derivative (or μ_i) are obtained from the Cubic-Plus-Association (CPA) EoS [9–13].

$$f_0 = -\rho RT - \rho RT\ln\left(\frac{p}{RT}\right) + RT\sum_{i=1}^{n_c}\rho_i\ln\rho_i - \frac{a\rho}{b}\ln(1+b\rho) - \rho RT\ln(1-b\rho) + RT\sum_{i=1}^{n_c}\rho_i\sum_{A_i}\left[\ln(X_{A_i}) - \frac{X_{A_i}}{2} + \frac{1}{2}\right] \tag{10}$$

$$\mu_i = -RT\ln(1-b\rho) - \frac{2}{b\rho}\ln(1+b\rho)\sum_{j=1}^{n_c}\rho_j\sqrt{a_ia_j}(1-k_{ij}) + \left\{\frac{RT\rho}{1-b\rho} + \frac{a}{b^2}\ln(1+b\rho) - \frac{a\rho}{b\ln(1+b\rho)}\right\}\cdots \times\left(\frac{1}{\rho}\sum_{j=1}^{n_c}\rho_j(b_i+b_j) - b\right) + RT\left\{\sum_{A_i}\ln(X_{A_i}) - \frac{1}{2\rho}\sum_{j=1}^{n_c}\rho_j\sum_{A_j}(1-X_{A_j})\frac{\partial\ln g}{\partial\rho_i}\right\} \tag{11}$$

In the latter equations, n_c is the number of components (here $n_c = 2$), p is the total pressure, R is the universal gas constant, T is the temperature. ρ is the molar density, ρ_i is the molar density of specie i. ρ_i and ρ are related by the mole fraction x_i according to $\rho_i = x_i\,\rho$. a and a_i are the cohesion parameter in the mixture, and for the pure specie i, respectively. b and b_i are the covolume of mixture, for the pure specie i, respectively. k_{ij} is the interaction parameter. X_{A_i} is the mole fraction of pure component i not bonded at site A and g is the simplified radial distribution function [36].

Both the mixture cohesion and covolume parameters are related to the corresponding pure component parameters by the following quadratic mixture rules:

$$\rho^2 a = \sum_{i=1}^{n_c}\sum_{j=1}^{n_c}\rho_i\rho_j\sqrt{a_ia_j}(1-k_{ij}) \tag{12.a}$$

$$\rho b = \sum_{i=1}^{n_c}\rho_i b_i \tag{12.b}$$

where the pure component cohesion parameter of CPA has a Soave-type reduced temperature ($T_r = T/T_c$) dependency:

$$a_i = a_{0,i}\left[1 + c_{1,i}\left(1 - \sqrt{T_r}\right)\right]^2 \tag{13}$$

The pure compound parameters ($a_{0,i}$, $c_{1,i}$, b_i) are regressed from selected pure component vapor pressure (p^0) and liquid density (ρ^{liq}) data. For the case of 2,5-Dimethylfuran, p^0 and ρ^{liq} data have been taken from Ref. [8] whereas p^0 and ρ^{liq} data for 2,2′-oxybis[propane] have been taken from the Daubert and Danner data base [35].

In Eqs. (10) and (11), X_{A_i} is related to the association strength $\Delta^{A_iB_j}$ between two sites belonging to two different molecules and is calculated by solving the following set of equations:

$$X_{A_i} = \left(1 + \sum_j\rho_j\sum_{B_j}X_{B_j}\left(\sqrt{\Delta^{A_iB_i}\times\Delta^{A_jB_j}}\right)\right)^{-1} \tag{14}$$

where the self-association $\Delta^{A_iB_i}$ is given by:

$$\Delta^{A_iB_i} = g(\rho)\left[\exp\left(\frac{\varepsilon^{A_iB_i}}{RT}\right) - 1\right]b_i\beta^{A_iB_i} \tag{15}$$

Table 2
Experimental vapor pressures p^0 as a function of temperature T for 2,2′-oxybis[propane] or DIPE.[a]

T (K)	p^0 (kPa)
307.64	30.01
311.53	35.01
314.98	40.01
318.08	45.01
320.94	50.01
323.56	55.01
326.00	60.01
328.29	65.01
330.45	70.01
332.48	75.01
334.41	80.01
336.23	85.01
339.65	95.01
341.52	100.89

[a] The measurement uncertainties are: $T \pm 0.02$ K, $p \pm 0.03$ kPa.

In Eq. (15), $\varepsilon^{A_iB_i}$ and $\beta^{A_iB_i}$ are the association energy and the association volume, respectively. $g(\rho)$ is the simplified radial distribution function [36], which is given by:

$$g(\rho) = \left(1 - \frac{19}{40} b\rho\right)^{-1} \quad (16)$$

In this work, pure fluids and mixture are considered non-associating fluids.

As we can observe, all the required SGT data input is obtained from pure fluid properties, and the CPA EoS. Henceforward, the SGT operates as a *full predictive scheme*.

4. Results and discussion

4.1. Vapor–liquid equilibrium

The experimental VLE or vapor pressures for DIPE, p_1^0, are reported in Table 2, whereas the corresponding p^0 values for DMF, p_2^0, have been previously reported elsewhere [8]. For DIPE and DMF, the temperature dependence of p_i^0 was correlated using the Antoine Eq. (4), where the corresponding A_i, B_i, C_i constants have been summarized in Table 3. In both cases, Eq. (4) correlated the vapor pressure data of the pure fluids within a maximum absolute percentage deviation (ADP) of 0.13%. Comparing the estimated vapor pressure of DIPE from Eq. (4) with the experimental vapor pressures of DIPE reported in Ref. [23], it is possible to conclude that the Antoine's parameters reported in Table 3 predict very well the experimental data reported in Ref. [23] with an ADP = 0.3%.

For the case of the binary system, the experimental VLE data for DIPE (1) + DMF (2) at p = 50, 75, and 94 kPa are reported in Tables 4–6, and depicted in Fig. 1. In these tables we have included the equilibrium temperature T, the liquid x_i and vapor y_i phase mole fractions of component i, the pure component (B_{ii} and B_{jj}) and cross (B_{ij}) second virial coefficients and the activity coefficients (γ_i) which were calculated from Eq. (2). The experimental data reported in Tables 4–6 indicates that the DIPE + DMF binary mixture exhibits a slight positive deviations from ideal behavior.

The VLE data reported in Tables 4–6 were found to be thermodynamically consistent by the point-to-point method of Van Ness et al. [29] as modified by Fredenslund et al. [30] For each isobaric condition, consistency criterion ($\Delta y < 0.01$) was met by fitting the equilibrium vapor pressure according to the Barker's [31] reduction method. Statistical analysis [37] revealed that a three parameters Legendre polynomial is adequate for fitting the equilibrium vapor pressure in each case. Pertinent consistency statistics and Legendre polynomial parameters are presented in Table 7 and its capability to correlate the VLE data are illustrated in Fig. 1.

In order to establish the capability of the CPA EoS for modeling the VLE data and then predict ST for the DIPE + DMF binary systems, the CPA EoS pure parameters ($a_{0,i}$, $c_{1,i}$, b_i) have been fitted by using the pure fluids vapor pressure (p^0) and molar liquid density (ρ^{liq})

Table 4
Experimental VLE data for 2,2′-oxybis[propane] or DIPE (1) + 2,5-Dimethylfuran or DMF (2) at p = 50.00 kPa.[a]

T (K)	x_1	y_1	γ_1	γ_2	$-B_{ij}$ (cm^3 mol^{-1})		
					11	22	12
345.24	0.000	0.000		1.000		1340	
343.13	0.050	0.121	1.172	0.996	1334	1363	1343
341.34	0.096	0.213	1.143	0.998	1352	1382	1361
339.86	0.134	0.285	1.143	0.998	1368	1398	1377
338.32	0.179	0.357	1.119	1.002	1384	1415	1394
336.70	0.231	0.434	1.109	1.000	1402	1434	1412
333.69	0.335	0.561	1.088	1.005	1436	1469	1446
332.03	0.396	0.623	1.079	1.012	1455	1489	1465
330.95	0.445	0.669	1.069	1.008	1467	1502	1478
329.69	0.499	0.714	1.060	1.014	1482	1517	1493
328.63	0.553	0.755	1.047	1.016	1495	1531	1506
327.52	0.601	0.789	1.046	1.023	1508	1545	1520
326.78	0.646	0.817	1.032	1.031	1518	1554	1529
324.85	0.750	0.880	1.024	1.034	1542	1580	1554
323.80	0.810	0.912	1.019	1.038	1555	1594	1567
322.85	0.869	0.941	1.013	1.046	1567	1607	1580
321.82	0.930	0.970	1.010	1.068	1581	1621	1593
321.03	1.000	1.000	1.000		1591		

[a] The measurement uncertainties are: $p \pm 0.03$ kPa; $T \pm 0.01$ K; $x_1, y_1 \pm 0.001$.

Table 5
Experimental VLE data for 2,2′-oxybis[propane] or DIPE (1) + 2,5-Dimethylfuran or DMF (2) at p = 75.00 kPa.[a]

T (K)	x_1	y_1	γ_1	γ_2	$-B_{ij}$ (cm^3 mol^{-1})		
					11	22	12
357.21	0.000	0.000		1.000		1225	
355.03	0.051	0.115	1.165	0.998	1220	1245	1228
353.00	0.097	0.214	1.192	0.995	1239	1264	1246
351.47	0.139	0.287	1.169	0.995	1253	1278	1261
349.93	0.185	0.358	1.140	0.996	1267	1293	1275
348.62	0.227	0.417	1.124	0.996	1280	1306	1288
347.19	0.274	0.478	1.115	0.996	1294	1320	1302
345.78	0.329	0.535	1.082	1.007	1307	1335	1316
343.67	0.396	0.614	1.097	1.000	1329	1357	1337
342.62	0.443	0.662	1.090	0.986	1339	1368	1348
341.54	0.496	0.702	1.066	0.998	1350	1380	1359
340.22	0.551	0.745	1.060	1.004	1364	1394	1373
338.83	0.601	0.784	1.068	1.006	1379	1409	1388
338.38	0.649	0.813	1.040	1.006	1384	1415	1393
336.00	0.755	0.878	1.040	1.022	1410	1442	1420
335.23	0.809	0.908	1.027	1.026	1418	1451	1428
334.17	0.870	0.939	1.021	1.044	1430	1463	1440
333.37	0.931	0.969	1.011	1.029	1439	1472	1450
332.65	1.000	1.000	1.000		1448		

[a] The measurement uncertainties are: $p \pm 0.03$ kPa; $T \pm 0.01$ K; $x_1, y_1 \pm 0.001$.

Table 3
Antoine coefficients (A_i, B_i and C_i) in Eq. (4).[a]

Compound	A_i	B_i	C_i	Temperature range (K)
2,2′-Oxybis[propane] or DIPE	6.03745	1182.9403	−48.2657	307.64–341.52
2,5-Dimethylfuran or DMF[a]	5.64673	1011.4342	−89.0388	331.46–366.79

[a] Parameters have been taken from Ref. [8].

Table 6
Experimental VLE data for 2,2′-oxybis[propane] or DIPE (1) + 2,5-Dimethylfuran or DMF (2) at p = 94.00 kPa.[a]

T (K)	x_1	y_1	γ_1	γ_2	$-B_{ij}$ (cm^3 mol^{-1})		
					11	22	12
364.37	0.000	0.000		1.000		1162	
362.32	0.046	0.103	1.185	0.999	1158	1180	1164
360.27	0.096	0.203	1.170	0.997	1175	1197	1182
358.83	0.133	0.272	1.174	0.992	1187	1210	1194
357.17	0.182	0.346	1.144	0.994	1201	1225	1208
355.55	0.230	0.414	1.130	0.996	1216	1240	1223
354.36	0.273	0.467	1.109	0.997	1226	1251	1234
353.55	0.295	0.493	1.108	1.003	1234	1258	1241
352.64	0.325	0.533	1.112	0.995	1242	1267	1250
350.69	0.394	0.604	1.100	1.000	1260	1286	1268
349.47	0.441	0.654	1.099	0.988	1272	1298	1279
348.22	0.496	0.700	1.086	0.989	1284	1310	1292
347.38	0.550	0.736	1.055	1.002	1292	1319	1300
346.27	0.596	0.771	1.054	1.003	1303	1330	1311
345.25	0.649	0.809	1.044	1.003	1313	1340	1321
344.00	0.704	0.845	1.043	1.008	1325	1353	1334
343.28	0.751	0.872	1.031	1.012	1332	1361	1341
342.32	0.806	0.903	1.023	1.022	1342	1371	1351
341.09	0.870	0.937	1.021	1.031	1355	1385	1364
340.13	0.931	0.968	1.014	1.022	1365	1395	1374
339.57	1.000	1.000	1.000		1371		

[a] The measurement uncertainties are: $p \pm 0.03$ kPa; $T \pm 0.01$ K; $x_1, y_1 \pm 0.001$.

Table 7
Consistency test statistics for the binary system 2,2′-oxybis[propane] or DIPE (1) + 2,5-Dimethylfuran or DMF (2).

P (kPa)	L_1[a]	L_2[a]	L_3[a]	$100 \times \Delta y$[b]	δP[c] (kPa)
50.00	0.1721	0.0242	0.0065	0.5	0.1
75.00	0.1836	0.0532	0.0034	0.8	0.3
94.00	0.1903	0.0346	0.0148	0.9	0.3

[a] Parameters for the Legendre polynomial [30] used in consistency.
[b] Average absolute deviation in vapor phase mole fractions $\Delta y = (1/N)\sum_{i=1}^{N} \left| y_i^{exp} - y_i^{cal} \right|$ (N: number of data points).
[c] Average absolute deviation in vapor pressure $\delta P = (1/N)\sum_{i=1}^{N} \left| P_i^{exp} - P_i^{cal} \right|$.

data. For the case of DIPE, both p^0 and ρ^{liq} were taken from the Daubert and Danner data base [35], whereas p^0 and ρ^{liq} for DMF were taken from our previous work [8]. Table 8 summarized the corresponding CPA EoS pure parameters as well as their Absolute Average Deviations (AAD). Once the pure fluid parameters have been defined; the VLE is calculated from Eqs. (7.a)–(7.c), where the interaction parameter k_{ij} was optimized from experimental data presented in Tables 4–6 with a value of $k_{ij} = -0.0075$. From Fig. 1, it is possible to observe that the CPA EoS model provides an excellent description of the VLE data. Based on these results, it is possible to conclude that the CPA EoS may be effectively used to describe the VLE of biofuels mixtures, as also previously shown for biodiesel and its derivatives [38–40] and, moreover it can also be used to predict the surface tensions of these systems as described below.

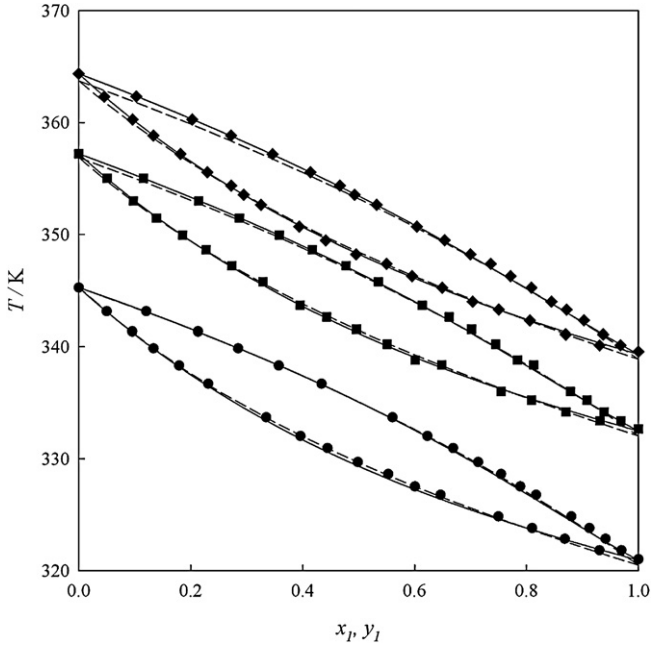

Fig. 1. Equilibrium temperature (T) as a function of the liquid (x_1) and vapor (y_1) mole fractions for the system 2,2′-oxybis[propane] or DIPE (1) + 2,5-Dimethylfuran or DMF (2). Experimental data at (●) 50.00 kPa; (■) 75.00 kPa; (♦) 94.00 kPa; (—) predicted from the three-parameter Legendre polynomial used in consistency analysis (Table 7); (– –) data results from CPA-EoS with pure compounds parameters indicated in Table 8, and $k_{ij} = -0.0075$.

Table 9
Surface tensions (σ) as a function of the liquid mole fraction (x_1) for the binary system 2,2′-oxybis[propane] or DIPE (1) + 2,5-Dimethylfuran or DMF (2) at 283.15 K and 101.3 kPa.[a]

x_1	σ (mN m^{-1})
0.000	26.34
0.067	24.79
0.112	24.27
0.234	23.31
0.323	22.56
0.420	21.87
0.520	21.31
0.626	20.86
1.000	18.88

[a] The measurement uncertainties are: $\sigma \pm 0.01$ mN m^{-1}; $T \pm 0.01$ K; $x_1 \pm 0.001$.

4.2. Surface tension and interfacial behavior

The atmospheric surface tension measurements for pure fluids and their mixture at 283.15 and 330.15 K are reported in Tables 9 and 10 and depicted in Figs. 2 and 3. In Fig. 2 we also included the reported experimental data [8,35] and the SGT correlation given by Eq. (8). The latter equation has been used to regress the influence parameters for the pure fluids (c_{11} and c_{22}). For both DMF and DIPE, a constant c_{ii} value is adequate to correlate

Table 8
CPA pure compound parameters (a_0, c_1, b) and influence parameters (c_{ii}) for the pure components.[a]

Fluid	a_0 (J m^3 mol^{-2})	c_1	10^5b (m^3 mol^{-1})	10^{20} c_{ii} (J m^5 mol^{-2})	%AAD[c]		
					p^0	ρ^{liq}	σ
2,2′-Oxybis[propane] or DIPE	2.472705	0.896753	11.5905	48.29697	2.38	0.59	0.56
2,5-Dimethylfuran or DMF	2.078484	1.004469	9.1824	30.64650	0.95	0.25	0.51

[a] Experimental data for vapor pressure (p^0), molar liquid density (ρ^{liq}), and surface tension (σ) have been taken from Daubert and Danner [35] for DIPE and from Mejía et al. [8] for DMF.
[b] The reduced temperature (T/T_c) ranges were the EoS parameters and influence parameters were fitted are: DIPE from 0.45 to 0.85 and DMF from 0.52 to 0.64.
[c] The Absolute Average Deviation AAD% $= (100/N)\sum_i^N \left| \delta_i^{exp} - \delta_i^{cal} \right| / \delta_i^{exp}$ with $\delta = p^0$, ρ^{liq}, or σ.

Table 10
Surface tensions (σ) as a function of the liquid mole fraction (x_1) for the binary system 2,2′-oxybis[propane] or DIPE (1) + 2,5-Dimethylfuran or DMF (2) at 330.15 K and 101.3 kPa.[a]

x_1	σ (mN m^{-1})
0.000	20.58
0.153	19.28
0.192	18.93
0.245	18.31
0.342	17.66
0.434	17.01
0.543	16.48
0.664	15.79
0.782	15.16
0.897	14.65
1.000	13.88

[a] The measurement uncertainties are: $\sigma \pm 0.01$ mN m^{-1}; $T \pm 0.01$ K; $x_1 \pm 0.001$.

ST for pure fluid in a broad range of temperature, as it is shown in Fig. 2. Table 8 summarizes the c_{ii} values and its absolute percentage deviation, where it is possible to observe that Eq. (8) correlated the ST data of the pure fluids within a maximum Absolute Average Deviation (AAP) of 0.56%.

Fig. 3 depicts the ST experimental data for the mixture. These data were also correlated using the Redlich–Kister expansion proposed by Myers and Scott [32] (see Eq. (5)). The corresponding parameters together with the correlation statistics are reported in Table 11. From the latter figure, it is possible to observe that the ST of DIPE (1) + DMF (2) exhibits negative deviations from the linear behavior ($x_1\sigma_1 + x_2\sigma_2$). In addition, it is possible to observe that, at a fixed isothermal condition, the σ decreases as the DIPE concentration increases, whereas at a fixed mole fraction σ decreases as the temperature increases.

Using the c_{ii} values previously described in Eq. (6), the ST *predictions* for the mixture are included in Fig. 3. The latter results clearly highlight the capability of a theoretically based model for predicting the surface tension in biofuels mixtures, as also previously shown when using the CPA equation of state coupled with the SGT to describe surface tensions of fatty acid esters and

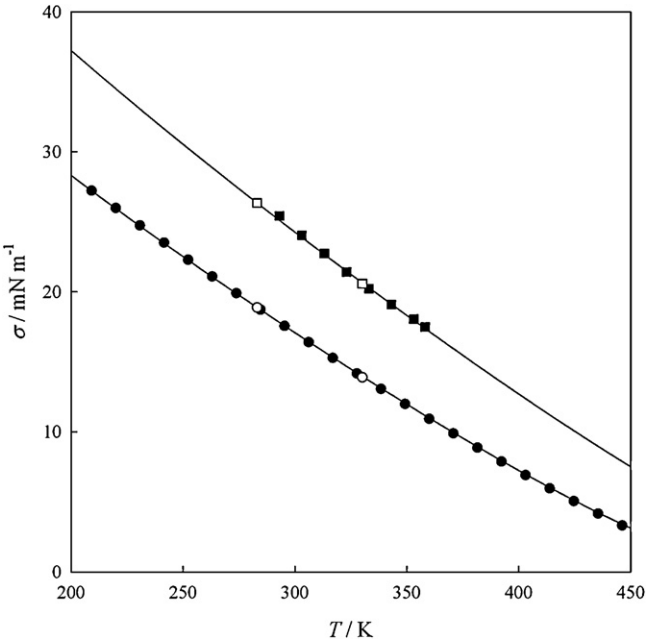

Fig. 2. Surface tension (σ) as a function of the temperature for pure fluids. (—) predicted from SGT–CPA-EoS with pure compounds parameters indicated in Table 8; 2,2′-oxybis[propane] or DIPE: (●) Daubert and Danner [35]; (○) this work. DMF: (■) Mejía et al. [8]; (□) this work.

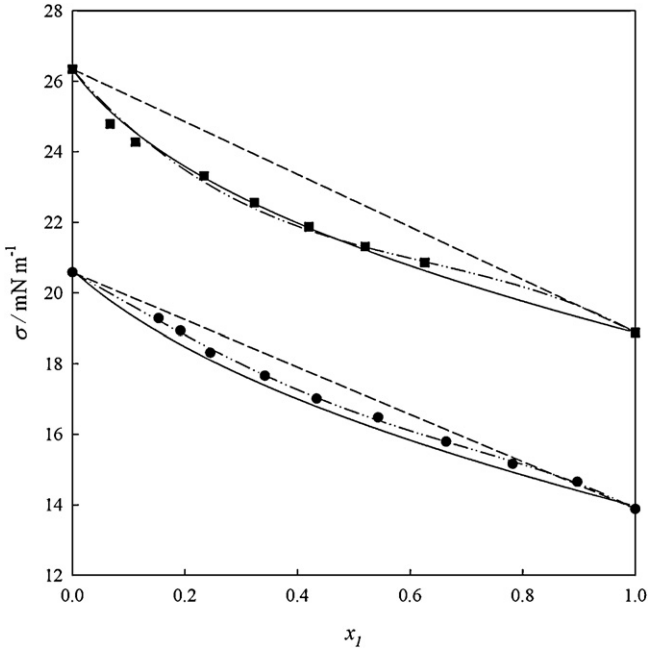

Fig. 3. Surface tension (σ) as a function of the liquid mole fraction (x_1) for the system 2,2′-oxybis[propane] or DIPE (1) + 2,5-Dimethylfuran or DMF (2) at 101.3 kPa and (■) 283.15 K; (●) 330.15 K; (– –) lineal behavior ($x_1\sigma_1 + x_2\sigma_2$); (–••–) smoothed by a Redlich–Kister expansion with the parameters shown in Table 11; (—) predicted from SGT–CPA-EoS with pure compound parameters indicated in Table 8, and $k_{ij} = -0.0075$.

commercial biodiesels in a wide range of temperatures [21,22]. This capability can also be used to analyze other interfacial properties such as the concentration population in the interface. Fig. 4 shows the interfacial profile in the $\rho_1 - \rho_2$ projection. From this figure, it is possible to observe that DIPE exhibits surface activity at the

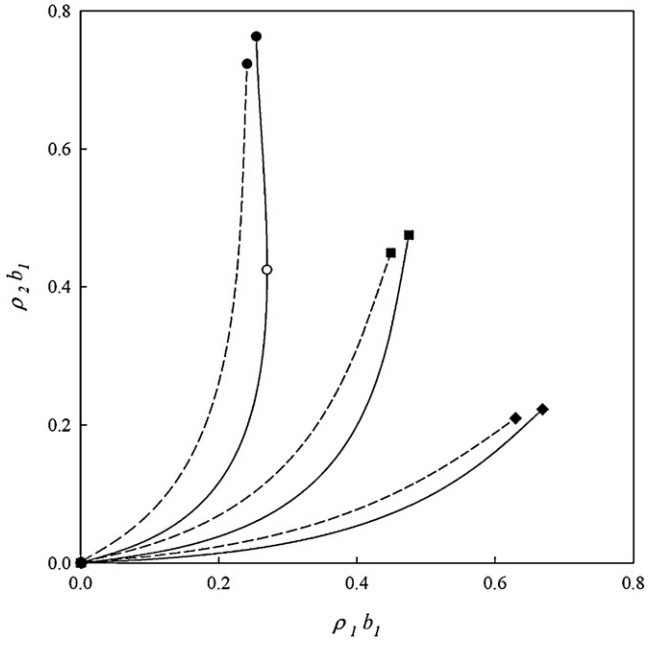

Fig. 4. Concentration profiles in the $\rho_1 - \rho_2$ projection at three liquid phase mole fractions (x_1) for the system 2,2′-oxybis[propane] or DIPE (1) + 2,5-Dimethylfuran or DMF (2) at 283.15 K, 330.15 K and 101.3 kPa. Predicted from SGT–CPA-EoS with pure compound parameters indicated in Table 8 (Eq. (9)): (—) 283.15 K; (– –) 330.15 K. Bulk densities: (●) $x_1 = 0.25$; (■) $x_1 = 0.50$; (♦) $x_1 = 0.75$. (○) stationary points ($d\rho_1/d\rho_2 = 0$).

Table 11
Coefficients (c_0, c_1, and c_2) and deviations (maximum (max dev), average (avg dev) and standard (st dev)) obtained in correlation of surface tension, Eq. (5), for the 2,2′-oxybis[propane] or DIPE (1) + 2,5-Dimethylfuran or DMF (2) at T and 101.3 kPa.

T (K)	c_0 (mN m^{-1})	c_1 (mN m^{-1})	c_2 (mN m^{-1})	max dev (10^3 mN m^{-1})	avg dev (10^3 mN m^{-1})	st dev (10^3 mN m^{-1})
283.15	−4.9108	−6.0630	0.0000	169.10	38.68	51.79
330.15	−2.3811	−1.8426	2.1591	13.95	3.23	4.10

interfacial region, denoted by the geometric condition where $d\rho_1/d\rho_2 = 0$. This surface activity implies that DIPE is accumulated in the interfacial region [15,33]. According to Fig. 4, the accumulation of DIPE decreases as the mole fraction of DIPE or temperature increases.

5. Conclusions

Vapor–liquid equilibrium and interfacial properties (concentration profile in the interfacial region, surface activity and surface tension) for the binary system DIPE + DMF have been described over the whole mole fraction range. According to experimental VLE results, the mixture exhibits slight positive deviation from the ideal behavior and does not present azeotropic behavior over the studied experimental range. The phase equilibrium data of the binary mixture satisfies the Fredenlund's consistency test. Surface tensions exhibit negative deviation from the linear behavior, and the experimental data were satisfactorily correlated using the Redlich–Kister equation. In addition to the new experimental data reported for the VLE and ST of the mixture, a full predictive theoretical scheme was used to predict both phase equilibrium and interfacial properties. The theoretical approach was based on SGT and the Cubic-Plus-Association equation of state. According to the results, accurate predictions of the experimental VLE and ST data were obtained, showing once again the capability of these models to be applied for biofuels mixtures. In addition, the present approach applied to a characterization of the interfacial behavior allows concluding that DIPE is adsorbed at the interface, and it decreases as the concentration of DIPE or temperature increases.

Funding sources

This work was financed by FONDECYT, Santiago, Chile (Project 1120228), and FCT–Fundação para a Ciência e a Tecnologia, through the project Pest-C/CTM/LA0011/2011. M.B.O. also acknowledges to postdoctoral grant SFRH/BPD/71200/2010.

References

[1] J.B. Binder, R.T. Raines, J. Am. Chem. Soc. 131 (2009) 1979–1985.
[2] Y. Romaïn-Leshkov, C.J. Barrett, Z.Y. Liu, J.A. Dumesic, Nature 447 (2007) 982–985.
[3] S. Zhong, R. Daniel, H. Xu, J. Zhang, D. Turner, M.L. Wyszynski, P. Richards, Energy Fuels 24 (2010) 2891–2899.
[4] X. Wu, Z. Huang, T. Yuan, K. Zhang, L. Wei, Combust. Flame 156 (2009) 1365–1376.
[5] R. Daniel, G. Tian, H. Xu, M.L. Wyszynski, X. Wu, Z. Huang, Fuel 90 (2011) 449–458.
[6] S.P. Verevkin, F.M. Welle, Struct. Chem. 9 (1998) 215–221.
[7] K.V. Auwers, Justus Liebigs Ann. Chem. 408 (1915) 212–284.
[8] A. Mejía, H. Segura, M. Cartes, J.A.P. Coutinho, J. Chem. Eng. Data 57 (2012) 2681–2688.
[9] I.V. Yakoumis, G.M. Kontogeorgis, E.C. Voutsas, E.M. Hendriks, D.P. Tassios, Ind. Eng. Chem. Res. 37 (1998) 4175–4182.
[10] G.M. Kontogeorgis, E.C. Voutsas, I.V. Yakoumis, D.P. Tassios, Ind. Eng. Chem. Res. 35 (1996) 4310–4318.
[11] E.C. Voutsas, G.C. Boulougouris, I.G. Economou, D.P. Tassios, Ind. Eng. Chem. Res. 39 (2000) 797–804.
[12] G.M. Kontogeorgis, G.K. Folas, Thermodynamic Models for Industrial Applications: From Classical and Advanced Mixing Rules to Association Theories, Wiley, UK, 2010.
[13] M.B. Oliveira, J.A.P. Coutinho, A.J. Queimada, Fluid Phase Equilib. 258 (2007) 58–66.
[14] J.D. van der Waals, Zeit. Phys. Chem. 13 (1893) 657–725 (see J.S. Rowlinson, J. Stat. Phys. 20 (1979) 197–244 for an English translation).
[15] A. Mejía, H. Segura, L.F. Vega, J. Wisniak, Fluid Phase Equilib. 227 (2005) 225–238.
[16] A. Mejía, H. Segura, J. Wisniak, I. Polishuk, J. Phase Equilib. Diffus. 26 (2005) 215–224.
[17] A. Mejía, H. Segura, M. Cartes, Fluid Phase Equilib. 308 (2011) 15–24.
[18] A. Mejía, H. Segura, M. Cartes, J. Ricardo Pérez-Correa, Fluid Phase Equilib. 316 (2012) 55–56.
[19] A.J. Queimada, C. Miqueu, I.M. Marrucho, G.M. Kontogeorgis, J.A.P. Coutinho, Fluid Phase Equilib. 228–229 (2005) 479–485.
[20] M.B. Oliveira, I.M. Marrucho, J.A.P. Coutinho, A.J. Queimada, Fluid Phase Equilib. 267 (2008) 83–91.
[21] M.B. Oliveira, J.A.P. Coutinho, A.J. Queimada, Fluid Phase Equilib. 303 (2011) 56–61.
[22] S.V.D. Freitas, M.B. Oliveira, A.J. Queimada, M.J. Pratas, A.S. Lima, J.A.P. Coutinho, Energy Fuels 25 (2011) 4811–4817.
[23] A. Mejía, H. Segura, M. Cartes, C. Calvo, Fluid Phase Equilib. 270 (2008) 75–86.
[24] J.D. Raal, D. Ramjugernath, in: R.D. Weir, Th.W. de Loos (Eds.), Measurement of the Thermodynamic Properties of Multiple Phases, vol. VII, Elsevier, Amsterdam, 2006.
[25] M.J.B. Evans, in: R.D. Weir, Th.W. de Loos (Eds.), Measurement of the Thermodynamic Properties of Multiple Phases, vol. VII, Elsevier, Amsterdam, 2006.
[26] H.C. Van Ness, M.M. Abbott, Classical Thermodynamics of Nonelectrolyte Solutions, McGraw-Hill Book Co., New York, 1982.
[27] H.G. Rackett, J. Chem. Eng. Data 15 (1970) 514–517.
[28] C. Tsonopoulos, AIChE J. 20 (1974) 263–272.
[29] H.C. Van Ness, S.M. Byer, R.E. Gibbs, AIChE J. 19 (1973) 238–244.
[30] A.a. Fredenslund, J. Gmehling, P. Rasmussen, Vapor–Liquid Equilibria Using UNIFAC, A Group Contribution Method, Amsterdam, Elsevier, 1977.
[31] J.A. Barker, Aust. J. Chem. 6 (1953) 207–210.
[32] D.B. Myers, R.L. Scott, Ind. Eng. Chem. 55 (1963) 43–46.
[33] B.S. Carey, L.E. Scriven, H.T. Davis, AIChE J. 24 (1978) 1076–1080 (Ibid., AIChE J. 26 (1980) 705–711).
[34] M. Modell, J. Tester, Thermodynamics and Its Applications, 3th ed., Prentice-Hall, New York, 1996.
[35] T.E. Daubert, R.P. Danner, Physical and Thermodynamic Properties of Pure Chemicals. Data Compilation, Taylor and Francis, Bristol, PA, 1989.
[36] G.M. Kontogeorgis, I.V. Yakoumis, H. Meijer, E. Hendriks, T. Moorwood, Fluid Phase Equilib. 160 (1999) 201–209.
[37] J. Wisniak, A. Apelblat, H. Segura, Phys. Chem. Liq. 35 (1997) 1–58.
[38] S.V.D. Freitas, M.B. Oliveira, A.S. Lima, J.A.P. Coutinho, Energy Fuels 26 (2012) 3048–3053.
[39] M.B. Oliveira, S. Miguel, A.J. Queimada, J.A.P. Coutinho, Ind. Eng. Chem. Res. 49 (2010) 3452–3458.
[40] M.B. Oliveira, V. Ribeiro, A.J. Queimada, J.A.P. Coutinho, Ind. Eng. Chem. Res. 50 (2011) 2348–2358.